Plasma broadening of Ne II–Ne VI and F IV–F V spectral lines

N. I. Uzelac,* S. Glenzer, N. Konjević,† J. D. Hey,‡ and H.-J. Kunze
Institut für Experimentalphysik V, Ruhr-Universität, 4630 Bochum, Germany
(Received 9 July 1992)

The Stark widths of 3*s*-3*p* and 3*p*-3*d* transitions of Ne II, Ne III, Ne IV, Ne V, Ne VI, F IV, and F V have been measured in the plasma of a gas-liner pinch discharge. The plasma parameters were determined from 90° Thomson scattering. Some of the measured Stark widths for Ne II, Ne III, and Ne IV lines are in good agreement with other experimental data. The results of three independent theoretical calculations are used for comparison with the measured widths. A growing discrepancy between theoretical and experimental results with increasing ionization is detected.

PACS number(s): 52.70.Kz, 32.70.Jz

I. INTRODUCTION

A large number of experimental papers is devoted to the study of Stark broadening of spectral lines (see, e.g., Ref. [1] and references therein). Unfortunately, most of the reported data relate to spectral lines of neutral atoms and positive ions of low ionization stages. In order to test various theoretical approximations, however, there is an urgent need for reliable experimental data for higher ionization stages.

Furthermore, a systematic discrepancy between theory and experiment which increases with ionization stage has recently been detected for the $3s\ ^2S$–$3p\ ^2P^\circ$ transitions of the Li-like ions C IV, N V, O VI, and Ne VIII [2]. In order to test this result, we have performed a systematic experimental study of analogous lines from low (singly ionized) to higher ionization stages (up to five times ionized neon). Isoelectronic transitions of F IV and F V are also studied.

Some of the investigated lines of Ne are potential candidates for laser transitions [3–6]. Therefore, the knowledge of the Stark broadening parameters for these lines is needed for calculations of radiative transfer in plasma sources of interest as active laser media.

II. THEORETICAL STARK WIDTHS

For the calculation of theoretical Stark widths a semiclassical approximation [Eq. (526) of Ref. [7]], a semiempirical formula plus modification [Eqs. (7)–(9) of Ref. [8]] put forth by Dimitrijević and Konjević (DK) and a classical-path approximation, which will be discussed in more detail below, have been used. Data for energy levels, where available, are taken from Refs. [9–12].

The first two theoretical models are derived for application to higher ionization stages (doubly, triply ionized, etc.), but for the sake of consistency, the modified semiempirical formula [8] has been used for the calculation of Ne II Stark widths, too.

Ion broadening by quadrupole interactions [Eq. 218(a) of Ref. [7]] is found to be of the order of 10% for our experimental conditions and we did not include this contribution in the linewidth since it is poorly known.

In the classical-path calculations of Hey and Breger for electron perturbers, denoted HB later in this paper, the effective Gaunt factors are determined within the impact approximation [13–16] without the use of semiempirical data. The main details of this method, which is derived for hyperbolic perturber trajectories of arbitrary curvature, have been described in the literature [17–20] (there denoted as Method I), and the computer program developed by Breger [21, 22] has been modified in order to improve the precision of the adiabatic cutoff to the impact parameter at the upper limit [16] as well as the method of averaging over the strong collision contributions. The need for upper and lower cutoffs to the impact parameter in these calculations is discussed below. Strong collision contributions are included for both upper and lower states of each line, but the upper-lower state interference term is set equal to zero. Another approach, which allows for the effects of adiabaticity and trajectory curvature without introducing an upper cutoff to the impact parameter, is described in Sec. II.3d of Ref. [7].

For each spectral line, a sufficiently complete set of perturbing levels (typically 40–90 per line) was prepared with the aid of available atomic data [9–12]. In order to achieve satisfactory values of the completeness parameter [17–21] (over 90%) for both the upper and the lower levels, many deficiencies in the published energy-level schemes [9–12] were supplemented with the aid of simple quantum-defect estimates or interpolations from isoelectronic ions. For reasons of speed and efficiency, all radial transition integrals have been evaluated by the Coulomb approximation [23], terms with equivalent outer (optical) electrons playing a very minor role in the broadening. By far the best energy-level data are now available for Ne III [12], while serious omissions still exist for the higher ionization stages. Possible errors in the estimation of the positions of many missing levels are one obvious source of inaccuracy in the calculations, since a comparatively small number of collision-induced transitions plays a major role in determining both the weak and the strong contributions to the linewidth [24, 25]. This in turn means that atomic structure effects for the radiator, such as configuration interaction [18, 26] and the transition from

pure LS to intermediate coupling [27–30], both of which are clearly evident in the comprehensive description of the Ne III atomic system [12], could influence the broadening through the line strengths which are contained in the expressions for the relevant collision strengths. Particularly useful in assessing such effects are the calculated purities of the LS level assignments in Ref. [12]. From these it could be shown that, while they certainly affect the outcome of the present work, the uncertainties caused by the simplification of treating the Ne III ion as purely LS coupled were reduced through the sum rules to a few percent. On the other hand, deviations from LS coupling are so serious in all but the s-p transitions in Ne II [31] that these cannot simply be ruled out as unimportant in accounting, to some extent, for the discrepancies evident in Table I (see Sec. IV). (The description of the $3p$-$3d$ transitions in the Ne II table of Ref. [32] was also found to be in conflict with the measured intensity ratios in the present experiment.) Information of sufficiently good quality is too fragmentary for most of the remaining ions to enable an assessment of the influence of such radiator structural effects to be made.

We turn now to a consideration of the effective Gaunt factor approximation for the calculation of weak collision contributions to the broadening. Its use implies that only the optically allowed collision-induced transitions (direct terms, without exchange) are included in the summation over the set of perturbing levels, the line strengths (as noted above) being evaluated in this work in pure LS coupling. A useful assessment of this approximation is presented in Ref. [33], while its accuracy at high perturber energies has been demonstrated by Seaton [34], whose expression for the Bethe limit coincides with that in the present work [17–20]. The use of this approximation is more problematic at lower energies, particularly in the evaluation of the elastic contributions to the broadening, which are obtained by application of the formulas in the energy region below threshold [35]. Although, in general, conformity with the quantum-mechanical prescription of Gailitis is achieved [36, 37], such extrapolation of classical-path formulas cannot be expected to represent an accurate average over the important below-threshold resonances. Useful insight into this question may be obtained from discussions in connection with the close-coupling calculations of Barnes [38] and Seaton [39–41], as well as the distorted-wave calculations of Hey and Blaha [28]. It is interesting to note, however, that in earlier comparisons between semiempirical [35, 42] and classical-path calculations [43] and measurements, the average agreement between calculation and experiment did not appear to depend strongly on the relative partition of the weak collision contributions into elastic and inelastic parts.

Finally, we comment briefly on the range of the impact parameter used in the calculations. The need for a lower cutoff arises on three grounds: in order to prevent violation of the classical-path assumption by quantum diffraction effects, the requirement that the monopole-dipole approximation for the perturbation potential remain valid, and the necessity to conserve flux in the scattering process (i.e., unitarity) [7, 17–21]. There are two possible grounds for the upper cutoff in our calculations: adiabaticity and Debye shielding. The first would apply when the time dependence of the interaction is too slow to induce atomic transitions, and where the atom would merely respond adiabatically to the changing perturber field [16]. This cutoff also ensures that it is valid to replace the classical-path perturbation Hamiltonian in the interaction picture by the simpler form as derived for the laboratory frame [17–20]. The possibility that Debye shielding provide a more stringent cutoff is examined in Ref. [20]. From Eqs. (34)–(36) of Ref. [20], one finds that the need to modify the upper cutoff as a result of Debye shielding should not arise for the lines under consideration until electron densities of some 5×10^{19} cm^{-3} are attained. The various expressions for the impact parameter cutoffs are derived for hyperbolic perturber trajectories of arbitrary curvature [17–21].

III. EXPERIMENT

A. Plasma source

The line profiles were investigated on the gas-liner pinch device developed at the Ruhr-Universität Bochum [44–46]. It resembles a large-aspect-ratio z pinch characterized by two independent gas-inlet systems. The first gas, the so-called driver gas (in our case hydrogen), is introduced through a fast-acting electromagnetic valve with an annular nozzle to form a hollow gas cylinder near the wall. When a 11.1-μF capacitor bank (25–35 kV) is discharged through the preionized gas (for preionization a 50-nF capacitor charged to 20 kV is discharged through 50 annularly mounted needles), a compressed plasma column results, 1–2 cm in diameter and 5 cm long.

Neon or a 10% mixture of SF_6 in hydrogen, called the test gas, is injected with the second fast valve system along the axis of the discharge tube. When the valves and the discharge are properly timed, the test gas is concentrated in the central part of the discharge where the plasma is rather homogeneous. In this way there are no cold boundary layers of the investigated test gas; this allows side-on observations through four ports in the midplane of the discharge tube without application of an Abel inversion process.

The features of the plasma source depend critically on the amounts of driver and test gas and their injection during the time of plasma generation; for this reason several discharge conditions had to be used for different ionic species. Plasma parameters reached on the axis of the discharge in the present experiments were between $0.94 < N_e < 2.85 \times 10^{18}$ cm^{-3} and $7.3 \times 10^4 < T_e < 3 \times 10^5$ K. For this range of plasma parameters no self-absorption of the investigated lines was detected, as was checked by comparing spectral line intensities within multiplets with known line ratios [32, 47].

B. Plasma spectroscopy

The experimental setup is shown in Ref. [47], and only a few details are given here.

The radiation from the plasma is imaged onto the entrance slit (50 μm wide) of a 1-m monochromator (Spex model 1704) with 1:1 magnification and $f/12$ collection optics. The detector head of the optical multichannel analyzer (OMA II) was mounted in the exit plane of the monochromator, and was operated in the pulse mode with a gate duration of 30 ns.

A 2400-lines/mm plane grating blazed at the wavelength of 240 nm, with reciprocal linear dispersion of 0.0102 nm/pixel in the first order, was used for recording Ne III–Ne VI spectral lines. For the investigation of Ne II lines we employed a grating with 1200 lines/mm, blazed at 1000 nm, using it in the third order, with a linear reciprocal dispersion of 0.0060 nm/pixel. For recording F IV, F V, and some Ne III spectral lines we used the same 1200 lines/mm grating in fourth order with a linear reciprocal dispersion of 0.0041 nm/pixel. Contributions to the line profiles from other orders could be eliminated using filters (UG5 and glass).

The wavelength sensitivity dependence of the detection system was calibrated for each wavelength range under investigation using a standard tungsten lamp, smoothing the averaged recorded spectra by the procedure of adaptive smoothing [48]. The wavelength calibration was done utilizing a Hg spectral lamp and Fe and Al hollow cathode lamps. The recorded apparatus profile of the detection system had a full width at half maximum (FWHM) of 4–5 pixels. Its contribution to the recorded profile was taken into account, as shown below.

For testing the reproducibility of the discharge the plasma continuum radiation at 520 nm was monitored with a photomultiplier mounted at the exit slit of a $\frac{1}{4}$-m monochromator. This signal was also used to control and to set the OMA gate and the time of the laser pulse to different phases of the discharge.

For obtaining spectra of different ionization stages it was necessary to change the combination of plasma parameters by varying the discharge parameters, and then to adjust the time of observation during the discharge to the optimum appearance of the investigated lines.

Checks had been made to make sure that the line radiation under investigation was emitted from the central part of the plasma with a homogeneous distribution of parameters; the procedure has been discussed in Ref. [2].

Line profiles recorded for the same plasma condition were averaged in order to improve the signal-to-noise ratio, and they were fitted by a Voigt function employing a least-square fitting procedure [49]. The Voigt function was the convolution of the measured apparatus profile, a Doppler profile calculated for the measured ion temperature, and a Lorentzian function with variable parameters for the Stark broadening. The fitting procedure included also variation of the continuum. Figure 1 shows two examples of profiles of recorded spectral lines along with their fits. The contributions of Doppler and apparatus widths to the overall widths of the spectral lines under investigation were between 10% and 30%.

Spectra obtained from discharges without test gas were used to eliminate the effects of impurity lines which did not originate from test ions. Multiplet components were fitted by independent profiles and their intensity ratios showed that no appreciable self-absorption of the investigated lines was present.

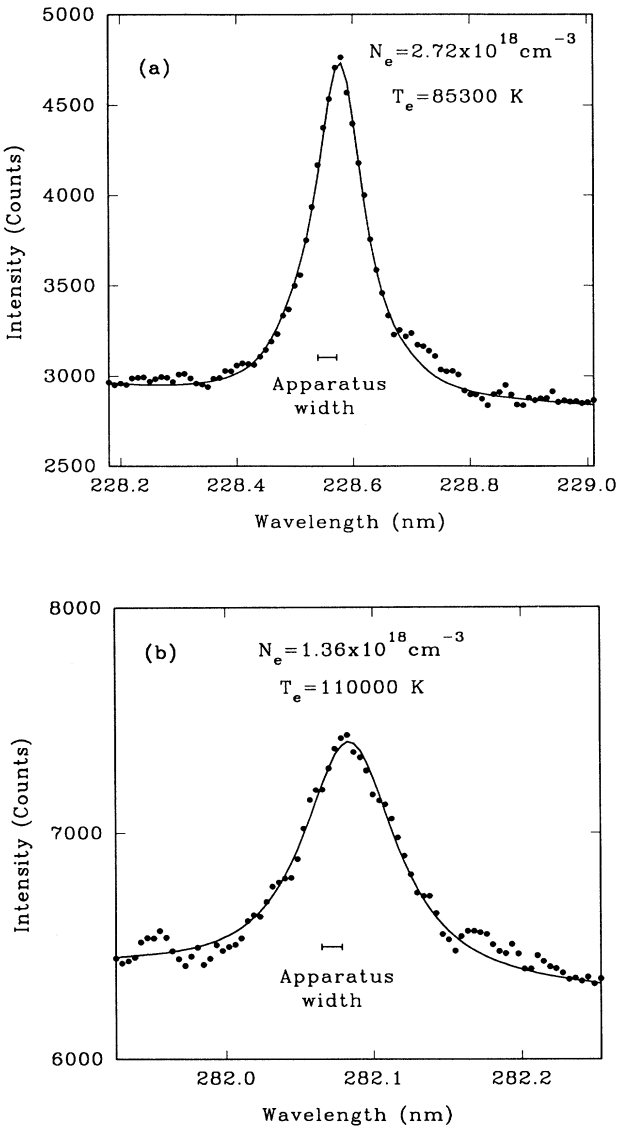

FIG. 1. Examples of recorded line spectra; · · ·, measured; —, Voigt function best fit. (a) Ne IV, (b) F IV. Electron densities and temperatures are obtained from Thomson scattering. The background is indicative of the high continuum radiation.

C. Plasma diagnostics

Electron densities and ion temperatures on the axis of the plasma were determined by 90° Thomson scattering [50]. An improved procedure of evaluating the Thomson scattering spectra was used, which is described in Ref. [2]. The Thomson scattering spectra were recorded with the detection system described above, using the 1200-lines/mm grating in second order (with the linear reciprocal dispersion of 0.0063 nm/pixel).

IV. RESULTS AND DISCUSSION

Experimental results for the Stark widths (FWHM) w_m of Ne II–Ne VI and F IV–F V lines are given in Table I together with plasma parameters and estimated errors for the various measured quantities. Stated uncertainties for electron densities and temperatures are rms values. Table I contains also spectroscopic data for the investigated lines and comparisons with theoretical results. The theoretical values w_G, w_{DK}, and w_{HB} are calculated according to Refs. [7, 8] and Sec. II of this paper, respectively.

In order to facilitate the comparison of our experimental results with other available experimental data obtained at different electron densities N_e, the average measured Stark widths w_m in Table II are normalized to $N_e = 1.0 \times 10^{17}$ cm^{-3}. We assumed a linear dependence of the Stark widths of the spectral lines of isolated nonhydrogenic ions upon electron density, as has been verified within experimental errors (for both widths and shifts) in a number of experiments (see, e.g., Refs. [1, 7, 51, 52]). As discussed above, Debye shielding of ion radiators from the influence of perturbing electrons is expected to play a minor role in the broadening under our plasma conditions. Therefore, scaling of experimental results to the same value of electron density should not introduce a large uncertainty into the comparison. Unfortunately, reliable investigations of the dependence of Stark widths on the electron temperature are almost completely missing, making scaling with electron temperature T_e rather uncertain. In order to take into account the $w(T_e)$ dependence in the comparisons in a appropriate way, ratios of average measured Stark widths w_m to the theoretical widths w_G, w_{DK}, and w_{HB} are given in Table II. In this way the theoretical dependence $w(T_e)$, which varies from one theoretical approach to the other, is introduced into the comparison. To illustrate this, the experimental

TABLE I. Experimental Stark widths w_m (FWHM) of investigated $3s$-$3p$ and $3p$-$3d$ transitions in Ne II–Ne VI and F IV–F V. Experimental results are compared with theoretical widths w_G calculated after Ref. [7], w_{DK} after Ref. [8], and w_{HB} (Sec. II).

Ion	Transition array	Multiplet (No.)	Wavelength (nm)	Temperature (10^4 K)	Electron density (10^{18}cm^{-3})	w_m (nm)	$\frac{w_m}{w_G}$	$\frac{w_m}{w_{DK}}$	$\frac{w_m}{w_{HB}}$
Ne II	$2p^4 3s$–$2p^4(^3P)3p$	^4P-$^4D^\circ$ (2)	333.484	7.3 ± 12%	1.90 ± 17%	0.120 ± 10%		1.11	0.59
				8.2 ± 5%	2.68 ± 17%	0.166 ± 8%		1.14	0.58
			336.063	7.3 ± 12%	1.90 ± 17%	0.100 ± 12%		0.93	0.48
				8.2 ± 5%	2.68 ± 17%	0.129 ± 12%		0.87	0.44
		^2P-$^2P^\circ$ (7)	332.374	7.3 ± 12%	1.90 ± 17%	0.146 ± 15%		1.20	0.63
			337.828	7.3 ± 12%	1.90 ± 17%	0.155 ± 15%		1.27	0.65
				8.2 ± 5%	2.68 ± 17%	0.151 ± 14%		0.91	0.45
	$2p^4 3p$–$2p^4(^3P)3d$	$^2D^\circ$-^4F (19)	336.720	7.3 ± 12%	1.90 ± 17%	0.184 ± 10%		1.03	0.46
				8.2 ± 5%	2.68 ± 17%	0.246 ± 12%		1.02	0.44
			338.846	7.3 ± 12%	1.90 ± 17%	0.216 ± 15%		1.21	0.53
				8.2 ± 5%	2.68 ± 17%	0.219 ± 15%		0.90	0.38
Ne III	$2p^3 3s$–$2p^3(^4S^\circ)3p$	$^5S^\circ$-^5P (11 UV)	259.000	8.5 ± 9%	2.72 ± 16%	0.093 ± 15%	0.70	1.15	0.87
			259.355	8.5 ± 9%	2.72 ± 16%	0.100 ± 15%	0.75	1.23	0.93
		$^3S^\circ$-^3P (12 UV)	267.790	8.5 ± 9%	2.72 ± 16%	0.114 ± 8%	0.74	1.23	0.90
	$2p^3 3s'$–$2p^3(^2D^\circ)3p'$	$^3D^\circ$-^3D	277.763	8.5 ± 9%	2.72 ± 16%	0.104 ± 5%	0.69	1.16	0.84
		$^3D^\circ$-^3F	261.006	8.5 ± 9%	2.72 ± 16%	0.106 ± 14%	0.79	1.31	0.95
		$^1D^\circ$-^1F	286.672	8.5 ± 9%	2.72 ± 16%	0.123 ± 5%	0.72	1.19	0.88
	$2p^3 3p'$–$2p^3(^2D^\circ)3d'$	^1F-$^1G^\circ$	227.358	8.5 ± 9%	2.72 ± 16%	0.078 ± 8%	0.56	1.09	0.76
	$2p^3 3s''$–$2p^3(^2P^\circ)3p''$	$^1P^\circ$-^1D	247.339	8.5 ± 9%	2.72 ± 16%	0.090 ± 11%	0.69	1.15	0.84
	$2p^3 3p''$–$2p^3(^2P^\circ)3d''$	^1D-$^1F^\circ$	250.704	8.5 ± 9%	2.72 ± 16%	0.107 ± 13%	0.60	1.15	0.80
Ne IV	$2p^2 3s$–$2p^2(^3P)3p$	^4P-$^4D^\circ$	235.252	8.5 ± 9%	2.72 ± 16%	0.079 ± 11%	0.97	1.33	1.15
			235.796	8.5 ± 9%	2.72 ± 16%	0.080 ± 11%	0.98	1.36	1.16
	$2p^2 3s'$–$2p^2(^1D)3p'$	^2D-$^2F^\circ$	228.579	8.5 ± 9%	2.72 ± 16%	0.076 ± 10%	0.96	1.36	1.15
			229.349	8.5 ± 9%	2.72 ± 16%	0.070 ± 18%	0.87	1.25	1.04
F IV	$2p3s$–$2p(^2P^\circ)3p$	$^3P^\circ$-^3D	282.074	12.2 ± 17%	0.94 ± 9%	0.050 ± 15%	1.13	1.61	1.32
				11.0 ± 20%	1.36 ± 11%	0.064 ± 9%	0.98	1.42	1.16
				16.7 ± 15%	1.57 ± 16%	0.072 ± 9%	1.03	1.56	1.18
Ne V	$2p3s$–$2p(^2P^\circ)3p$	$^3P^\circ$-^3D	226.571	29.8 ± 29%	2.85 ± 10%	0.064 ± 13%	1.28	1.71	1.32
F V	$2s2p3s$–$2s2p(^3P^\circ)3p$	$^4P^\circ$-^4D	270.230	16.7 ± 15%	1.57 ± 16%	0.071 ± 18%	1.39	1.90	1.52
Ne VI	$2s2p3s$–$2s2p(^3P^\circ)3p$	$^4P^\circ$-^4D	225.322	29.1 ± 24%	2.05 ± 17%	0.057 ± 8%	1.88	2.32	1.86
				29.8 ± 29%	2.85 ± 10%	0.072 ± 10%	1.78	2.22	1.70

TABLE II. Comparisons of average measured (w_m) and calculated [w_G [7], w_{DK} [8], and w_{HB} (Sec. II)] Stark widths at electron density $N_e = 1 \times 10^{17}\text{cm}^{-3}$ for Ne II, Ne III, and Ne IV lines. (Pres. denotes present work.)

Ion	Transition array	Multiplet (No.)	Temperature (10^4 K)	$w_m/(N_e \times 10^{-17})$ (10^{-1} nm)	$\frac{w_m}{w_G}$	$\frac{w_m}{w_{DK}}$	$\frac{w_m}{w_{HB}}$	Ref.
Ne II	$2p^4 3s$–$2p^4(^3P)3p$	^4P-$^4D^\circ$	2.8	0.161		1.83	1.41	[53]
		(2)	2.7	0.147		1.66	1.28	[54]
			3.0–4.0	0.117–0.102		1.38	0.96	[55]
			7.3	0.056		1.02	0.54	pres.
			8.2	0.055		1.00	0.51	pres.
		^2P-$^2P^\circ$	2.8	0.136		1.38	1.06	[54]
		(7)	3.0–4.0	0.130–0.147		1.37–1.78	1.02–1.16	[55]
			7.3	0.079		1.24	0.64	pres.
			8.2	0.056		0.91	0.49	pres.
	$2p^4 3p$–$2p^4(^3P)3d$	$^2D^\circ$-^4F	3.0-3.5	0.161–0.163		1.12–1.23	0.73–0.75	[55]
		(19)	7.3	0.105		1.12	0.50	pres.
			8.2	0.087		0.96	0.41	pres.
Ne III	$2p^3 3s$–$2p^3(^4S^\circ)3p$	$^5S^\circ$-^5P	3.4	0.050	0.79	1.10	1.15	[56]
		(11 UV)	8.5	0.035	0.73	1.19	0.90	pres.
		$^3S^\circ$-^3P	3.4	0.065	0.90	1.25	1.27	[56]
		(12 UV)	8.5	0.042	0.74	1.23	0.90	pres.
	$2p^3 3s'$–$2p^3(^2D^\circ)3p'$	$^3D^\circ$-^3D	3.4	0.054	0.77	1.07	1.07	[56]
			8.5	0.038	0.69	1.16	0.84	pres.
		$^3D^\circ$-^3F	3.4	0.047	0.75	1.04	1.04	[56]
			5.9	0.044	0.82	1.34	1.04	[57]
			8.5	0.039	0.79	1.31	0.95	pres.
Ne IV	$2p^2 3s$–$2p^2(^3P)3p$	^4P-$^4D^\circ$	5.9	0.032	0.86	1.25	1.19	[57]
			8.5	0.029	0.98	1.35	1.16	pres.
	$2p^2 3s'$–$2p^2(^1D)3p'$	^2D-$^2F^\circ$	5.9	0.029	0.89	1.20	1.11	[57]
			8.5	0.028	0.92	1.31	1.10	pres.

Stark widths normalized to $N_e = 1.0 \times 10^{17}$ cm^{-3} for Ne II $3s\ ^4P$–$3p\ ^4D^\circ$ transitions are given in Fig. 2, together with semiclassical results from Table V of Ref. [7], those obtained from the modified semiempirical formula [8] and from the classical-path approximation (see Sec. II).

Comparison of other experimental data with our experiment shows good agreement, well within the estimated uncertainties. The largest discrepancy was detected for Ne II $3s\ ^4P$–$3p\ ^4D^\circ$ lines, see Table II and Fig. 2. We observed Ne II lines in the recombination phase of the discharge when the Ne III lines disappear. This should ensure that Ne II ions are also distributed homogeneously in the plasma column. Although the agreement is within the error bars, the spread of experimental data in Fig. 2 is rather large. To clarify the $w(T_e)$ dependence in this case, a new experiment in the low-temperature region would be very desirable.

The comparison between our experiment and the theories [7, 8] and Sec. II, see Table I, shows that the theoretical results are in agreement with the experiment to within the estimated uncertainties of both the theories (±50%) and the experiment, with the exception of the Ne VI values. However, the systematic change of the ratio of experimental and theoretical results from lower to higher ionization stage may be an indication of inadequacy in the theories. The simplified semiclassical results (after Ref. [7]) show better agreement at higher ionization stages, while the modified semiempirical formula [8]

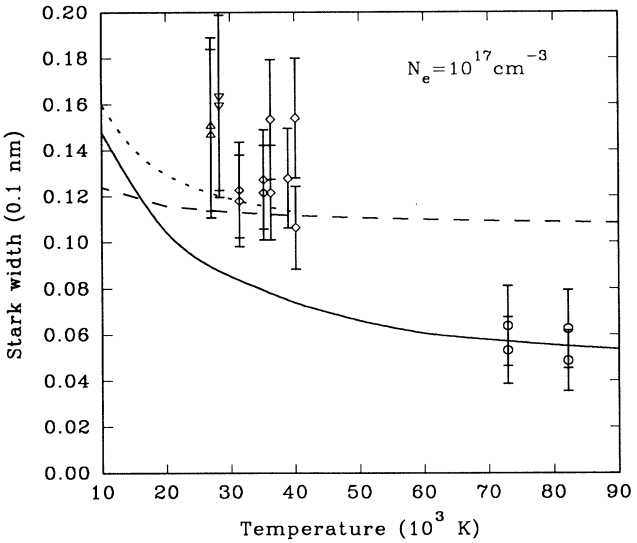

FIG. 2. Comparison of Stark width data for the Ne II $3s\ ^4P$–$3p\ ^4D^\circ$ lines. Experimental results: ∇, Ref. [53]; △, Ref. [54]; ◇, Ref. [55]; ○, present results. Error flags include authors' uncertainty estimates in both half-width and electron density measurements. Theoretical results: · · ·, semiclassical after Ref. [7], Appendix V; —, evaluated from a modified semiempirical formula [8]; - - -, classical-path approximation (Sec. II).

seems to be better suited for the low ionization stages. Calculations performed as discussed in Sec. II give values which lie between those two.

In order to determine whether an undetected systematic error in our experiment had influenced the comparison with the theory, other experimental results along the isoelectronic sequence of carbon for the $2p3s - 2p(^2P^\circ)3p$ triplet transitions are shown in a comparison given in Table III. The systematic change of the ratio of experimental to theoretical values shows a similar trend as detected in Table I and in Ref. [2]. Unfortunately, all results for higher ionization stages (Tables I and III and Ref. [2]) are obtained with the same plasma source and the same experimental procedure. It would be desirable, therefore, to have results from other plasma sources and with other diagnostic techniques before drawing a final conclusion on the discrepancy between experiments and theories.

V. THEORETICAL CONSIDERATIONS

While the calculated results on the whole fall within the total (random plus systematic) error limits associated with the measurements in the case of the Ne III–Ne V and the F IV lines, agreement in the case of Ne II is unexpectedly poor, especially in the light of earlier success with the present method [17–19, 43] (also evident in the better agreement with other measurements listed in Table II). Apart from atomic structure considerations mentioned above (see Sec. II), it should be mentioned that the approximate treatment of the strong collision contributions should not be expected to influence the results in such a major way in the case of Ne II, the strong collision contributions being under 20% in all cases. Only a much stronger temperature dependence in the calculations would enable all sets of data in Table II to be satisfied simultaneously. The reader might note that our strong collision contributions for singly charged radiators are appreciably smaller than typical values tabulated in Ref. [7], which are in turn quoted from Ref. [66]. This may perhaps be understood in the following way: in this calculation [66], the authors make no explicit distinction between elastic and inelastic contributions to the broadening, and thus part of the role of the inelastic term has been taken up by their "strong" contribution to the line widths. Indeed, the demarcation between "strong" and "weak" in Ref. [66] is described there as being "somewhat arbitrary." A more explicit partition into elastic and inelastic contributions was later made in Ref. [67], which represents a further development of the treatment in Ref. [68].

Apart from the somewhat anomalous case of Ne II, the general deterioration (systematic increase in the ratio $w_m/w_{\rm th}$) in going from lower to higher ionization stages remains to be discussed. Explanations for these observations could be attempted in the following terms: the general deterioration in the validity of the impact approximation with increasing ratio of density to temperature, the possible need to include higher-order multipole series contributions to the interaction energy, the increasing importance of the optically forbidden collision-induced transitions in higher-Z ions, the need to refine the expression for the strong collision contribution, and far more significant contributions from ion perturbers than have been allowed for here. In addition, the role that highly curved trajectories in the Kramers limit [16, 69] might play in invalidating the lower impact parameter cutoff, and the effect of dielectronic satellites in dense, colder, recombining plasmas [70] (the latter, however, producing significant asymmetries which are absent here) have been considered. The role of highly curved trajectories as a possible source of error in classical-path calculations

TABLE III. Comparisons of average measured (w_m) and calculated Stark widths (w_G after Ref. [7] and $w_{\rm DK}$ after Ref. [8]) for N II, O III, F IV, and Ne V ions [$2p3s - 2p(^2P^\circ)3p$ transition of carbon sequence, triplets]. The values for $3kT/2|\Delta E|$ represent the ratio of the thermal electron energy to the energy difference with the nearest perturbing level.

Ion	Multiplet	w_m/w_G	$w_m/w_{\rm DK}$	$3kT/2\|\Delta E\|$	Ref.
N II	$^3P^\circ$-^3D		1.22	2.14	[58]
	$^3P^\circ$-^3P		1.32	1.36	[59]
			1.12	1.41	[60]
			0.79	1.00	[61]
			1.13	1.43	[62]
			1.32	2.23	[58]
			0.76	3.28	[63]
	$^3P^\circ$-^3S		1.94	1.89	[58]
O III	$^3P^\circ$-^3D	0.78	1.03	1.65	[64]
	$^3P^\circ$-^3P	0.82	1.09	1.67	[64]
		1.04	1.46	2.68	[65]
	$^3P^\circ$-^3S	0.89	1.24	2.68	[65]
F IV	$^3P^\circ$-^3D	1.05	1.53	3.33	present expt.
Ne V	$^3P^\circ$-^3D	1.28	1.71	4.71	present expt.

was estimated as of minor importance in Ref. [66], and is also considered in Ref. [68]. We comment briefly on the four major lines of attack.

The impact approximation, a major cornerstone of this calculation, is in fact a high-velocity, low-density approximation, and its validity for such plasmas as considered here should therefore be verified. Validity criteria derived earlier [19, 20] are, however, comfortably satisfied in all cases. Nevertheless, these criteria may be too optimistic on quantum-mechanical grounds: Barnes [38] long ago considered the possibility that the perturbing electron, on striking a resonance, be temporarily captured before autoionization occurs, thus introducing a time delay which could invalidate the impact approximation. He was able to show that, for the singly charged ions under consideration, the impact approximation remains valid even in the resonance regions. This effect, which of course cannot be calculated in the classical-path approximation, may conceivably play a greater role for the high-Z ions in environments where fulfillment of the necessary criteria is in any case more critical. Proper consideration of optically forbidden collision-induced transitions [24] is again facilitated by quantum-mechanical calculations. Some interesting features are also seen in the work of Hey and Blaha [28] for singly ionized radiators, notably unexpectedly high monopole and quadrupole (predominantly monopole) contributions to the broadening. One might again anticipate that the monopole terms would increase in importance with Z, their role in the strong collision contributions to the shifts, for example, having already been shown to be dominant [71]. The need to refine the relatively crude strong collision term has been suggested in the literature [22, 72]. Although this is clearly desirable, the question may also be asked whether the simple demarcation into strong and weak collision regimes does not require a further degree of refinement. A concrete example of what different calculations yield for the relative contributions to the broadening may be of interest to the reader at this point. Calculations of the hydrogenic C VI line at 343.4 nm by Kepple and Griem [67] yield, for typical plasma conditions of interest, roughly the following: broadening by ion perturbers, 67%; broadening by electron perturbers, 15% strong (total), 6% weak elastic, 12% weak inelastic. For the case of Ne VI we have for our conditions typically electron impact broadening, 50% strong (total), 3% weak elastic, 47% weak inelastic. The latter values are in reasonable conformity with earlier findings for O VI [2].

Finally, it is plausible that the ion perturbers could play a far more important role [72] than the comparatively simple estimates used here suggest.

It is clear that the present study has left many questions related to the broadening of ion lines unanswered, but may serve as a stimulus for new approaches to some old problems in spectral line broadening.

VI. CONCLUSIONS

We have reported results of Stark width measurements of isolated spectral lines of Ne II, Ne III, Ne IV, Ne V, Ne VI, F IV, and F V in the plasma of the gas-liner pinch. Our results are compared with other available experimental data and theoretical results calculated by the simplified semiclassical [7], modified semiempirical [8], and a classical-path (see Sec. II) approximation. Although other experiments were performed at different electron temperatures, thus complicating the comparison, the agreement is good and well within the estimated uncertainties (especially for $Z = 3$ and $Z = 4$). The largest discrepancy is detected for the Ne II $3s\,^4P$–$3p\,^4D^\circ$ transition; see Fig. 2. A comparison with the theoretical results [7, 8] and Sec. II of this paper shows agreement within the estimated uncertainties of both theory and experiment. However, a systematic change of the ratio of the experimental and theoretical results from one ionization stage to another is detected. To resolve this systematic discrepancy, further work, both experimental and theoretical, is required.

ACKNOWLEDGMENTS

This research was supported by the Sonderforschungsbereich 191 of the DFG. One of us (N.I.U.) wishes to express his gratitude to the Commission of the European Communities for financing his research stay at the Ruhr-Universität Bochum. The authors appreciate helpful comments by H. R. Griem and W. L. Wiese.

* Also at Institute of Physics Belgrade, 11080 Belgrade, Yugoslavia.
† Also at Faculty of Physics, University of Belgrade, 11001 Belgrade, Yugoslavia.
‡ Also at Institut für Plasmaphysik, Forschungszentrum Jülich GmbH, 5170 Jülich, Germany.

[1] N. Konjević and W. L. Wiese, J. Phys. Chem. Ref. Data **19**, 1307 (1990).
[2] S. Glenzer, N. I. Uzelac, and H.-J. Kunze, Phys. Rev. A **45**, 8795 (1992).
[3] P. K. Cheo and H. G. Cooper, J. Appl. Phys. **36**, 1862 (1965).
[4] W. B. Bridges and A. N. Chester, Appl. Opt. **4**, 573 (1965).
[5] J. B. Marling, J. Quantum Electron. **11**, 822 (1975).
[6] Y. Hashino, Y. Katsuyama, and K. Fukuda, Jpn. J. Appl. Phys. **11**, 907 (1972).
[7] H. R. Griem, *Spectral Line Broadening by Plasmas* (Academic, New York, 1974).
[8] M. S. Dimitrijević and N. Konjević, J. Quant. Spectrosc. Radiat. Transfer **24**, 451 (1980).
[9] C. E. Moore, *Atomic Energy Levels*, Natl. Bur. Stand. Ref. Data Ser., Natl. Bur. Stand. (U.S.) Circ. No. 35 (U.S. GPO, Washington, DC, 1971), Vol. II.
[10] S. Bashkin and J. O. Stoner, Jr., *Atomic Energy Levels and Grotrian Diagrams* (North-Holland, Amsterdam, 1975), Vols. I and II.
[11] R. L. Kelly, J. Phys. Chem. Ref. Data Suppl. 1 **16**, 141

(1987).
[12] W. Persson, C.-G. Wahlström, L. Jönsson, and H. O. Di Rocco, Phys. Rev. A **43**, 4791 (1991).
[13] M. Baranger, Phys. Rev. **111**, 481 (1958).
[14] M. Baranger, Phys. Rev. **111**, 494 (1958).
[15] M. Baranger, Phys. Rev. **112**, 855 (1958).
[16] M. Baranger, in *Atomic and Molecular Processes*, edited by D. R. Bates (Academic, New York, 1962), Chap. 13.
[17] J. D. Hey and P. Breger, J. Quant. Spectrosc. Radiat. Transfer **24**, 349 (1980).
[18] J. D. Hey and P. Breger, J. Quant. Spectrosc. Radiat. Transfer **24**, 427 (1980).
[19] J. D. Hey and P. Breger, in *Spectral Line Shapes*, edited by B. Wende (de Gruyter, Berlin, 1981), pp. 191–200.
[20] J. D. Hey and P. Breger, S. Afr. J. Phys. **5**, 111 (1982).
[21] P. Breger, M. Sc. thesis, University of Cape Town, 1980 (unpublished).
[22] F. Böttcher, P. Breger, J. D. Hey, and H.-J. Kunze, Phys. Rev. A **38**, 2690 (1988).
[23] J. D. Hey, S. Afr. J. Phys. **10**, 118 (1987).
[24] J. D. Hey, J. Quant. Spectrosc. Radiat. Transfer **17**, 729 (1977).
[25] J. D. Hey, J. Quant. Spectrosc. Radiat. Transfer **20**, 403 (1978).
[26] J. D. Hey and P. Breger, J. Quant. Spectrosc. Radiat. Transfer **23**, 311 (1980).
[27] J. D. Hey, J. Quant. Spectrosc. Radiat. Transfer **17**, 721 (1977).
[28] J. D. Hey and M. Blaha, J. Quant. Spectrosc. Radiat. Transfer **20**, 557 (1978).
[29] J. D. Hey, S. Afr. J. Phys. **8**, 27 (1985).
[30] T. L. Pittman and N. Konjević, J. Quant. Spectrosc. Radiat. Transfer **36**, 289 (1986).
[31] R. H. Garstang, Mon. Not. R. Astron. Soc. **114**, 118 (1954).
[32] W. L. Wiese, M. W. Smith, and B. M. Glennon, *Atomic Transition Probabilities*, Natl. Bur. Stand. Ref. Data Ser., Natl. Bur. Stand. (U.S.) Circ. No. 4 (U.S. GPO, Washington, DC, 1966), Vol. I.
[33] S. M. Younger and W. L. Wiese, J. Quant. Spectrosc. Radiat. Transfer **22**, 161 (1979).
[34] M. J. Seaton, Adv. At. Mol. Phys. **11**, 83 (1975).
[35] H. R. Griem, Phys. Rev. **165**, 258 (1968).
[36] M. Gailitis, Zh. Eksp. Teor. Fiz. **44**, 1974 (1963) [Sov. Phys. JETP **17**, 1328 (1963)].
[37] O. Bely, Phys. Rev. **185**, 79 (1969).
[38] K. S. Barnes, J. Phys. B **4**, 1377 (1971).
[39] M. J. Seaton, J. Phys. B **20**, 6363 (1987).
[40] M. J. Seaton, J. Phys. B **20**, 6431 (1987).
[41] M. J. Seaton, J. Phys. B **21**, 3033 (1988).
[42] J. D. Hey and R. J. Bryan, J. Quant. Spectrosc. Radiat. Transfer **17**, 221 (1977).
[43] J. D. Hey, A. Gawron, X. J. Xu, P. Breger, and H.-J. Kunze, J. Phys. B **22**, 241 (1989).
[44] K. H. Finken and U. Ackermann, Phys. Lett. **85A**, 278 (1981).
[45] K. H. Finken and U. Ackermann, J. Phys. D **15**, 615 (1982).
[46] H.-J. Kunze, in *Spectral Line Shapes*, edited by R. J. Exton (Deepak, Hampton, VA, 1987), Vol. 4.
[47] S. Glenzer, J. Musielok, and H.-J. Kunze, Phys. Rev A **44**, 1266 (1991).
[48] S. Kawata and S. Minami, Appl. Spectrosc. **38**, 49 (1984).
[49] J. E. Dennis, Jr. and D. J. Woods, in *New Computing Environments: Microcomputers in Large-Scale Computing*, edited by A. Wouk (SIAM, Philadelphia, 1987).
[50] A. Gawron, S. Maurmann, F. Böttcher, A. Meckler, and H.-J. Kunze, Phys. Rev. A **38**, 4737 (1988).
[51] N. Konjević and W. L. Wiese, J. Phys. Chem. Ref. Data **5**, 259 (1976).
[52] N. Konjević, M. S. Dimitrijević, and W. L. Wiese, J. Phys. Chem. Ref. Data **13**, 619 (1984).
[53] M. Platiša, M. S. Dimitrijević, and N. Konjević, Astron. Astrophys. **67**, 103 (1978).
[54] N. Konjević and T. L. Pittman, J. Quant. Spectrosc. Radiat. Transfer **35**, 473 (1986).
[55] J. Purić, S. Djeniže, A. Srećković, J. Labat, and Lj. Ćirković, Phys. Rev. A **35**, 2111 (1987); A. Srećković (private communication).
[56] N. Konjević and T. L. Pittman, J. Quant. Spectrosc. Radiat. Transfer **37**, 311 (1987).
[57] J. Purić, S. Djeniže, A. Srećković, M. Ćuk, J. Labat, and M. Platiša, Z. Phys. D **8**, 343 (1988).
[58] S. T. Purcell and A. J. Barnard, J. Quant. Spectrosc. Radiat. Transfer **32**, 205 (1984).
[59] H. F. Berg, W. Ervens, and B. Furch, Z. Phys. **206**, 309 (1967).
[60] N. W. Jalufka and J. P. Craig, Phys. Rev. A **1**, 221 (1970).
[61] N. Konjević, V. Mitrović, Lj. Ćirković, and J. Labat, Fizika **2**, 129 (1970).
[62] M. Popović, M. Platiša, and N. Konjević, Astron. Astrophys. **41**, 463 (1975).
[63] J. Purić, A. Srećković, S. Djeniže, and M. Platiša, Phys. Rev. A **36**, 3957 (1987).
[64] M. Platiša, M. Popović, and N. Konjević, Astron. Astrophys. **45**, 325 (1975).
[65] J. Purić, S. Djeniže, A. Srećković, and J. Labat, Phys. Rev. A **37**, 498 (1988).
[66] W. W. Jones, S. M. Benett, and H. R. Griem, University of Maryland Technical Report No. 71-128, 1971 (unpublished).
[67] P. C. Kepple and H. R. Griem, Phys. Rev. A **26**, 484 (1982).
[68] H. R. Griem, M. Blaha, and P. C. Kepple, Phys. Rev. A **19**, 2421 (1979).
[69] J. D. Hey and P. Breger, J. Phys. B **22**, L79 (1989).
[70] K. N. Koshelev, J. Phys. B **21**, L593 (1988).
[71] H. Nguyen, M. Koenig, D. Benredjem, M. Caby, and G. Coulaud, Phys. Rev. A **33**, 1279 (1986).
[72] A. Calisti, F. Khelfaoui, R. Stamm, B. Talin, and R. W. Lee, Phys. Rev. A **42**, 5433 (1990).